Materials Today: Proceedings xxx (xxxx) xxx

Contents lists available at ScienceDirect

Materials Today: Proceedings

journal homepage: www.elsevier.com/locate/matpr

The effect of process parameters on mechanical characteristics of specimens obtained via DLP additive manufacturing technology

Roberto Brighenti [a], Liviu Marsavina [b,*], Mihai P. Marghitas [b], Matteo Montanari [a], Andrea Spagnoli [a], Farzad Tatar [a]

[a] Department of Engineering and Architecture, University of Parma, Parma, Italy
[b] Department of Mechanics and Strength of Materials, University Politehnica Timisoara, Timisoara, Romania

ARTICLE INFO

Article history:
Available online xxxx

Keywords:
Additive Manufacturing
Digital Light Processing (DLP)
Fracture Toughness
Photopolymerization

ABSTRACT

Digital Light Process (DLP) is one of the Additive Manufacturing (AM) methods to produce three-dimensional (3D) polymeric components with high dimensional stability. The technique is based on light-induced polymerization, consisting in spreading the light of a suitable wavelength in a spatially controlled area according to the component's digital model. Starting from a liquid monomer solution, a 3D solid polymeric object is created. The mechanical and fracture properties of such components are highly influenced by the process parameters which must be carefully considered when load bearing parts have to be produced by AM. This paper investigates the effect of the DLP process parameters on tensile properties using dog bone specimens and fracture toughness determined by using Single Edge Notch Specimens loaded in three-point bending. Five different process parameters were considered by testing six specimens; for each of them, the influence of the printing orientation on the fracture toughness of UV-sensitive resin "translucent green" (curing UV light wavelength 405 nm) is considered. Among the various parameters, the study considers also the post-processing effects on the fracture toughness.

1. Introduction

Additive Manufacturing (AM) technologies have completely renewed the production processes in the last decades, allowing to obtain parts of complex geometry with precisions not achievable with traditional manufacturing technologies such as machining, cast, and molding [1].

AM technologies operate by adding layer-by-layer or small volume-by-small volume material elements to obtain the final part. The production possibilities offered by AM and the wide range of printable materials (metals, metal alloys, ceramics, plastics, etc.), offer endless possibilities to be exploited in many fields such as automotive [2], aerospace, electronics, healthcare and biomedical applications [3], smart and composite materials [4], etc., to mention just a few.

Among the 3D printing technologies, several have been developed to print polymers by adopting different approaches, such as by using filament deposition, laser sintering, and monomer resin solidification. In particular, the AM technologies exploiting the solidification of an initial liquid monomer resin through a light-induced polymerization reaction, allows us to produce elements with a very high geometrical resolution, down to 20–25 μm. It is based on a chemical-physical process that operates by solidifying, through the light of proper wavelength (typically UV light with a wavelength in the range 300–400 nm), a photopolymer initially in the liquid state [5–7]. Photopolymerization is used in the Stereolithography (SLA) technology where a moving light beam inducing the polymerization is cast on the liquid resin bath; more recently, the so-called Digital Light Processing (DLP) technology, which operates by directly projecting the UV-light image of the entire cross-section of the object being printed, has been developed.

In the present research, the effects of exposure time to the UV light, the thickness of the printed layers (which are often the main AM parameters to be set), as well as the printing direction on the final mechanical properties are experimentally studied.

* Corresponding author.
E-mail address: liviu.marsavina@upt.ro (L. Marsavina).

https://doi.org/10.1016/j.matpr.2023.01.092

It is illustrated that different choices of the above-mentioned parameters entail different mechanical properties of the final printed polymer; in particular, the influence of the AM setting parameters on Young's modulus, the tensile strength, and the fracture toughness are considered.

The fracture toughness of 3D printed specimens was determined for different AM technologies like Fused Deposition Modeling (FDM) [8–11] and Selective Laser Sintering (SLS) [12–13]. However, up to date, there have not been many studies regarding the fracture toughness of 3D printed specimens using DLP technology.

2. The physics of photopolymerization

Photopolymerization-based AM technologies involve various coupled chemical-physics phenomena that need to be properly described in order to obtain the final characteristics of the obtained printed material. In this section, we briefly summarize the main phenomena involved in the AM process based on the solidification of a photosensitive monomer.

2.1. Light diffusion

Since the polymerization process is triggered by light (with a proper wavelength), we need first to describe the light diffusion within a semi-transparent medium. Typically, a UV light beam hits the surface of the liquid bath and spreads inside the fluid domain; its intensity decreases as it enters the medium. The so-called Beer-Lambert law properly describes such a phenomenon [14]. The light diffusion equation and the related Dirichlet boundary conditions are as follows:

$$\boldsymbol{l}(\boldsymbol{X},t)\cdot\nabla_{\boldsymbol{X}} I(\boldsymbol{X},t) = -A(\boldsymbol{X},t)\, I(\boldsymbol{X},t) \quad \text{for } \boldsymbol{X}\in\Omega_0$$

$$I(\boldsymbol{X},t) = I_0(\boldsymbol{X},t) \quad \text{for } \boldsymbol{X}\in\partial\Omega_0 \tag{1}$$

being $I(\boldsymbol{X},t)$ the light intensity at the position $\boldsymbol{X}=(\mathrm{X},\mathrm{Y},\mathrm{Z})$ and time t, $\boldsymbol{l}(\mathrm{X},\mathrm{t})$ the unit vector of the light beam, $\nabla_{\boldsymbol{X}}$ is the gradient operator, while $A(\boldsymbol{X},t)$ is the absorbance of the material quantifying the light attenuation as it travels across the semi-transparent medium. In real problems, $A(\boldsymbol{X},t)$ is usually not constant because of its dependence on the concentration of the chemical species and on the degree of solidification of the polymer, making the problem highly non-linear.

2.2. Kinetics of chemical species evolution during photopolymerization

The light crossing the material is absorbed by photo-initiators and, in general, by other light reactive species present in the liquid monomer bath. This induces the liquid (monomers) → solid (polymer chains) conversion. In brief, the photo-chemical process is as follows: light radiation induces the conversion of the photo-initiator molecules into free radicals that react with monomer molecules leading to functional groups constituting the growing chains forming the backbone of the polymer [15].

The light-induced polymerization consumes the monomer molecules in the liquid bath and allows the polymer chains to form; the degree of monomer → polymer conversion is usually defined by the degree of cure (DOC) ϱ [16,18]:

$$\varrho(t) = 1 - C_M(t) {C_M}_0^{-1} \tag{2}$$

being $C_{M_0} = C_M(t=0)$ the initial concentration of the monomer molecules. Finally, the DOC ϱ can be related to the number of chains per unit volume (concentration of chains) $c_a(t)$ as [17]:

$$c_a(t) = \frac{\mu(\boldsymbol{X},t)}{k_B T} = \begin{cases} \frac{1}{3\,k_B T}\left\{E_d + E_c exp\left[s\left(\varrho(t)-\varrho_{gel}\right)\right]\right\} & \text{if } \varrho(t) > \varrho_{gel} \\ 0 & \text{if } \varrho(t) \le \varrho_{gel} \end{cases} \tag{3}$$

which is related in turn to the standard shear modulus μ of the material through the classical rubber-elasticity relationship $\mu = c_a k_B T$, being k_B, T the Boltzmann constant and the absolute temperature. ϱ_{gel} is the degree of cure corresponding to the monomer liquid starting to solidify, while E_c, E_d, s are fitting parameters. By indicating with $\bar{\mu} = k_B T\, \bar{c}_a = k_B T\, c_a(t\to\infty)$ the maximum achievable value of the shear modulus (fully cured polymer obtained by adopting a long time exposure to light), the c_a-ϱ relationship is alternatively given by:

$$c_a(t) = \underbrace{\left(\frac{\bar{\mu}}{k_B T}\right)}_{\bar{c}_a} \cdot \exp\left[\alpha(\varrho(t)-1)\right] \tag{4}$$

Finally, it is worth recalling that the chain concentration rate is provided by $\dot{c}_a(t) = \alpha\, \bar{c}_a\, \dot{\varrho}(t)$ and can be used to evaluate the current chain concentration by time integration, $c_a(t_c) = c_{a0} + \int_0^{t_c} \dot{c}_a(t)\, dt$, where the time interval $0 \div \mathrm{t_c}$ indicates the exposure or curing time.

In the following, the effect of the DLP process parameters on the tensile properties (true stress- stretch response, tensile strength, shear modulus) and the fracture toughness, determined using Single Edge Notch Specimens loaded in three-point bending, are presented. Samples were made from UV-sensitive resin "translucent green" (curing UV light wavelength 405 nm).

3. Effects of the printing parameters on the mechanical response of AM DLP polymers

Since the molecular-scale structure of a DLP AM material depends on the way the additive process has been performed, it is of crucial importance to understand how the final mechanical properties depend on the printing parameters. When photopolymerized-based AM technologies are considered for a given photopolymer, the main settings available to the user are related to the layer thickness, the exposure time, and the printing direction. The main goal of a DLP printing procedure is to obtain the most homogeneous and tough possible material to maximize the mechanical performance of the final part. In particular, the curing time is of crucial importance since it determines the polymer chain density and consequently the mechanical properties. However, the layer thickness also influences the degree of polymerization since the light intensity must be as high as possible during the UV exposure and large layer thicknesses do not promote a good monomer-polymer conversion.

Beyond the above-mentioned aspects, also the transparency of the material – both the liquid as well as in the solid state – plays a crucial role in the solidification process; low values of the absorbivity in the liquid and in the solid state enhance the light to enter the material by maintaining a sufficiently high intensity to promote the polymer chains formation; moreover, a good material transparency in the solidified state allows the material underneath the layer being cured, to be further cured and so polymerized.

From the above discussion appears that the photopolymerization-based AM technologies, if properly tuned and controlled, offer huge opportunities to tailor the properties of the final material with a simple and ad hoc setting of the printing process, achieving high-quality geometrical parts with mechanical properties suitable to the application of interest. In

the following, an experimental campaign performed to quantitatively understand the role played by the above-mentioned AM parameters on the main mechanical performances of an AM material is illustrated.

4. Experimental tests

4.1. Printing setup and characteristics of the AM specimens

The influence of the DLP photopolymerization parameters on the mechanical characteristics of AM printed parts is now considered by studying both the tensile properties as well as fracture toughness. Several specimens, printed by using UV-sensitive resin "translucent green" (curing UV light wavelength 405 nm) by varying the curing exposure time and the layer thickness, have been mechanically tested. A 3D LCD printer (Anycubic Photon® and anycubic wash and post-cure machine 2.0®) has been used to prepare the specimens.

The printed specimens have been prepared according to the following parameters: light exposure time has equal to $t_c = 10, 20, 30$ and 60s for each layer (curing UV light wavelength 405 nm), layer thickness set to the following values: $h_i = 0.03, 0.05, 0.07$ mm (Fig. 1). The geometry of the AM specimens and the testing procedure (determination of the tensile properties of plastics) has been assumed in accordance with the ISO 527-1 code [19]. Moreover, the influence of the printing direction has also been considered when studying the fracture toughness. Six specimens have been tested for each photopolymerization setting.

Static tensile tests have been performed by using a universal testing machine Galdabini Quasar 2.5 by adopting a displacement rate equal to $\dot{\delta} = 5$ mm/min, corresponding to a stretch rate $\dot{\lambda} \cong 0.018\ s^{-1}$. The tensile strength and the tangent elastic modulus vs the applied deformation have been determined for all the AM photopolymerization setups. The used photoresins are characterized by an absorbivity value equal to $A = 304\ m^{-1}$. The absorbivity has been determined by measuring the light intensity before (I_a) and after (I) crossing a part with a given thickness (h = 3 ÷ 6 mm) obtained by using different exposure times (10 ÷ 60 s). The absorbance has been calculated by using the solution of the one-dimensional Beer-Lambert diffusion equation, $A = [\ln(I_a) - \ln(I)]/h$; the absorbance resulted to be practically independent of the curing time, indicating that the solidification degree does not affect significantly the transparency of the material. The light intensity of the DLP printer has been measured to be equal to about $I_0(t) = 7.321 \cdot 10^{-4}\ mW/cm^2$.

The fracture toughness tests were performed according to ASTM D 5045-14 [20] using Single Edge Notched Specimens (SENB) with the following dimensions: width $W = 12$ mm, thickness $B = 6$ mm, crack length $a = 5$ mm and span $S = 4W = 48$ mm. Three printing directions (0°, 45°, and 90°, Fig. 2) were considered and three different post-printing curing treatments named: P5 – 5 min maintained in Isopropyl Alcohol (IPA) and then cured for 5 min, P4 – cleaned in hot water (60–70 °C) and 30 min ultrasonic curing, respectively cleaned for 5 min maintained in IPA and 30 min ultrasonic curing and P6 – 5 min maintained in Isopropyl Alcohol (IPA) and 30 min ultrasonic curing. The thickness layer was 0.05 mm, and the exposure time was 20 s for all SENB specimens.

The notch was printed during the 3D printing process and a crack was introduced with a razor blade. Tests were performed at room temperature with a loading speed of 2 mm/min. The load was applied statically, continuously and smoothly.

4.2. Static tensile test results

The influence of the printing parameters, namely the exposure time and the layer thickness, on the mechanical properties of DLP AM specimens has been considered first. In Fig. 3a the static tensile response of the material cured for $t_c = 30s$ is shown for a maximum tensile elongation equal to $\lambda = 1.02, 1.05$; a clear material degradation appears to occur even for low values of the applied deformation.

By evaluating the elastic modulus when the curing time t_c increases, it is reasonable to extrapolate the value of the shear modulus related to the case of the fully cured material to be equal to about $\bar{\mu} = 210\ MPa$. In Fig. 3b, c the dimensionless tensile strength and the dimensionless tangent Young's modulus vs the curing time, with the respective standard deviations, are illustrated; it is clear that the curing time t_c has a crucial effect on the elastic constant and on the tensile strength since their values increase upon increasing the time of exposure to the UV light. Further, the tensile strength of the material is slightly dependent on the layer thickness when the longest exposure time is concerned

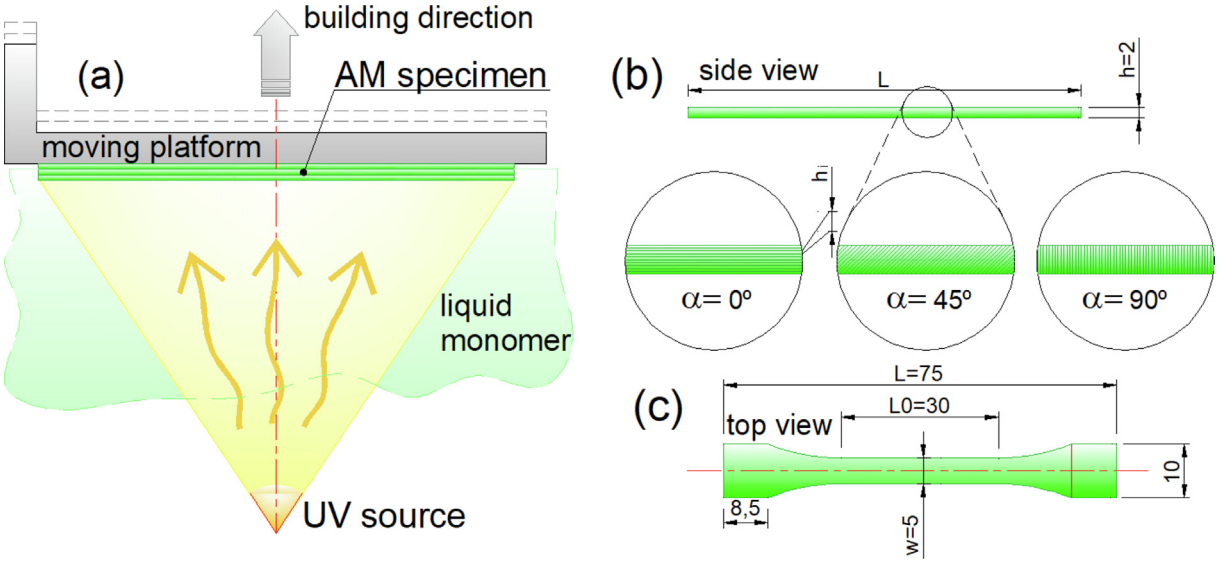

Fig. 1. Schematic of the DLP printing process (a). Details of the printing direction and layer thickness (b). Geometric sizes of the standard tensile specimens (c).

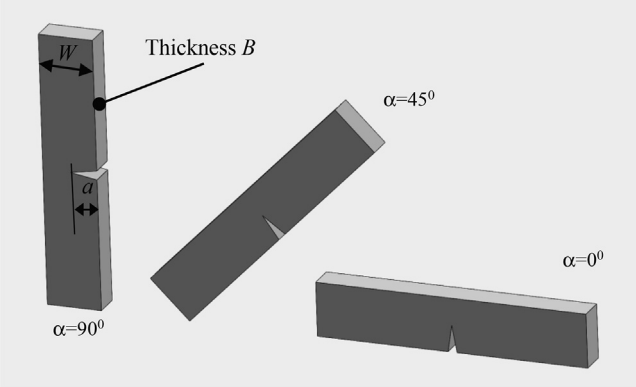

Fig. 2. Single Edge Notched Specimens used for fracture toughness tests and adopted printing orientations.

($t_c = 60$ s); on the other hand, shorter exposure times (t_c = 10 ÷ 30 s) provide lower strengths and the influence of the layer thickness appears to be more pronounced.

4.3. Fracture toughness results

The effect of the printing direction α as well as of the post curing treatment on the fracture toughness is considered in the present section, while the layer thickness and the exposure time have been kept constant and equal to 20 s, respectively.

A brittle fracture was observed for all tested specimens, which indicate that the fracture toughness K_{IC} represents an important material property for this type of components.

The fracture toughness was estimated according with ASTM D 5045-14 [19]:

$$K_{IC} = \frac{P_{max}}{B\ W^{0.5}} f\left(\frac{a}{W}\right), \tag{5}$$

where P_{max} represents the maximum load, B, W and a specimen dimensions, the non-dimensional Stress Intensity Factor (SIF) $f(a/W)$ was calculated based on specimen width and crack length:

$$f\left(\frac{a}{W}\right) = 6\left(\frac{a}{W}\right)^{0.5} \times \frac{\left[1.99 - \frac{a}{W}\left(1-\frac{a}{W}\right)\left(2.15 - 3.93\frac{a}{W} + 2.7\left(\frac{a}{W}\right)^2\right)\right]}{\left(1+2\frac{a}{W}\right)\left(1-\frac{a}{W}\right)^{1.5}} \tag{6}$$

The fracture toughness results are shown in Fig. 4, while in Fig. 5 are presented the average fracture toughness results.

It could be observed that the maximum mode I fracture toughness was obtained for 0° specimen orientation and for post curing treatment in IPA 5 min, followed by 5 min curing (1.311 $MPa\sqrt{m}$). The fracture toughness decreases with the printing orientation resulting in a minimum value of 0.382 $MPa\sqrt{m}$ for 90° orientation, which is justified by the arrangement of the printed layers parallel to the crack plane, a situation in which the crack propagation is enhanced by the weaknesses of the layer interfaces [21]. The other two post-printing curing treatments, namely *P*4 and *P*6, lead to lower values of the fracture toughness. The scatter of data for printing angle 0° could be attributed to the adhesion between layers [22].

The plain strain condition was verified for all specimens by using the so-called *P.S.C.* parameter, which – in order the plane strain condition to be fulfilled – should be higher than 1; it is defined as:

$$P.S.C. = \frac{B}{2.5\left(\frac{K_{IC}}{UTS}\right)^2} > 1 \tag{7}$$

In Eq. (7), the thickness B of the specimens (Fig. 2) is used because $a < B$ for all the investigated specimens.

The results of *P.S.C.* for 0° specimen orientation and different post-printing curing treatments are plotted in Fig. 6. The results show that the plain strain condition is fulfilled for all specimens, all orientations and all post-printing curing treatments, which confirms the brittle behaviour of the DLP printed specimens.

5. Conclusions

In the present study we studied experimentally the effect of the exposure time to UV curing light and the layers' thickness of a DLP printed photoresin polymer on some relevant mechanical properties, namely the tensile properties (elastic modulus and tensile strength) and the fracture toughness. It has been found that increasing the time exposure to the UV light plays a relevant role in improving the elastic properties and the strength of the material; setting small layers thickness is also important to improve the tensile properties, especially for the longest exposure times. The use of too large layer thickness does not lead to high mechanical tensile properties because of the limited polymerization taking place in the material due to its limited transparency which does not allow the light to penetrate deep into the material.

Dealing with the fracture toughness, it has been found that its value in DLP specimens is strongly affected by the printing orientation and also by the post printing curing process. Brittle behaviour was observed for all tested specimens and the plane strain condition was fulfilled. Thus, it can be concluded that the Linear Elastic Fracture Mechanics applies to these types of materials.

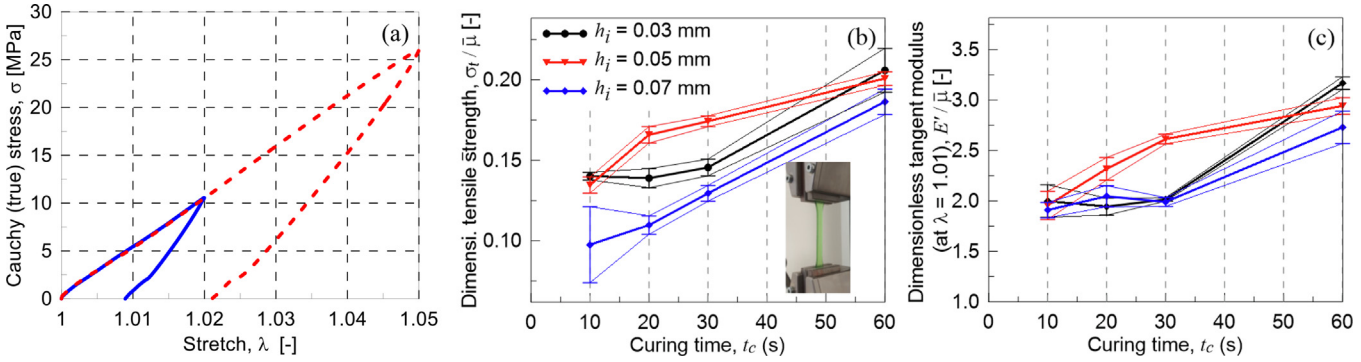

Fig. 3. Tensile loading cycles at 2% and 5% max deformation (a). Dimensionless mean tensile strength (b) and mean tangent Young's modulus (c) (at $\lambda = 1.01$) vs curing time for different layer thicknesses (h_i = 0.03, 0.05, 0.07 mm). Standard deviation ranges of the measured quantities are indicated with thin lines.

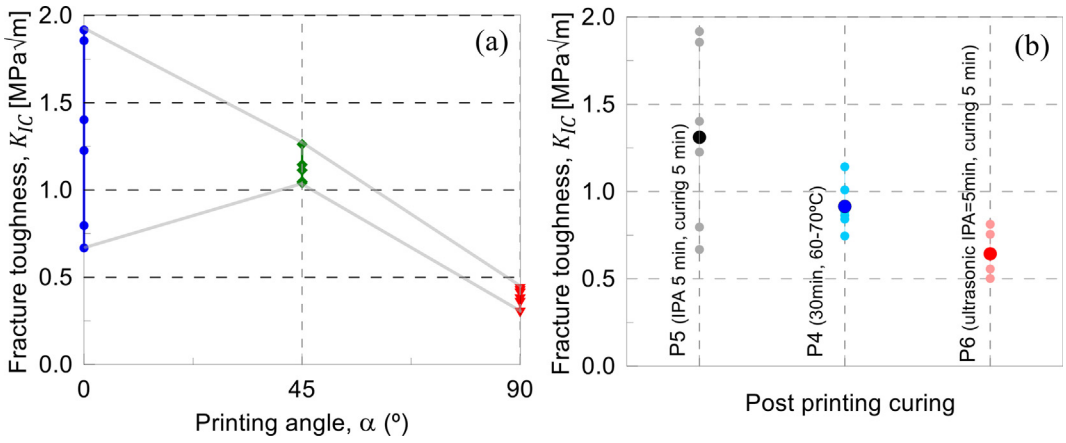

Fig. 4. Influence of printing orientation (a) and of the post printing curing procedure on the fracture toughness (b).

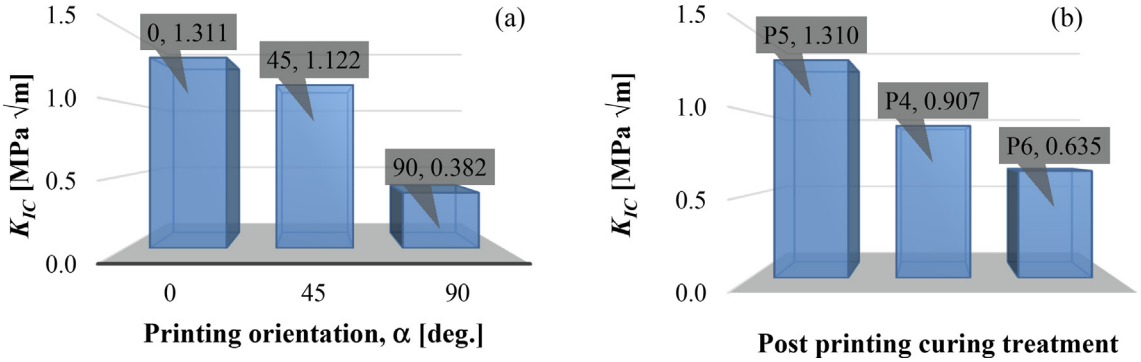

Fig. 5. Influence of printing orientation (a) and post curing treatment (b) on the average fracture toughness.

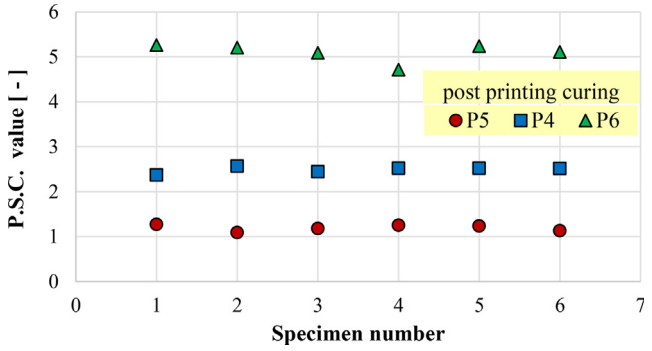

Fig. 6. Verification of the plain strain condition for the tested specimens.

From the experimental results, obtained by adopting different settings of the additively manufactured DLP photo-sensible polymeric materials, it can be concluded that the additive manufacturing of load-bearing polymeric parts requires a particular attention to the process setting and to the printing layout since they can strongly affect the final mechanical characteristics.

CRediT authorship contribution statement

Roberto Brighenti: Conceptualization, Methodology, Writing – original draft. **Liviu Marsavina:** Conceptualization, Methodology, Writing – review & editing. **Mihai P. Marghitas:** Investigation. **Matteo Montanari:** Investigation, Formal analysis. **Andrea Spagnoli:** Validation, Supervision. **Farzad Tatar:** Investigation.

Data availability

Data will be made available on request.

Declaration of Competing Interest

The authors declare that they have no known competing financial interests or personal relationships that could have appeared to influence the work reported in this paper.

Acknowledgement

The project leading to these results has received funding from the European Union's Horizon 2020 research and innovation program (H2020-WIDESPREAD-2018, SIRAMM) under grant agreement No. 857124 and was supported by a grant of the Romanian Ministry of Education and Research, CNCS/CCCDI - UEFISCDI, project number PN-III-P3-3.6-H2020-2020-0079.

References

[1] H. Bikas, P. Stavropoulos, G. Chryssolouris, Additive manufacturing methods and modelling approaches: a critical review, Int. J. Adv. Manuf. Technol. 83 (2016) 389–405, https://doi.org/10.1007/s00170-015-7576-2.
[2] R. Leal, F.M. Barreiros, L. Alves, F. Romeiro, J.C. Vasco, M. Santos, C. Marto, Additive manufacturing tooling for the automotive industry, Int. J. Adv. Manuf. Technol. 92 (5) (2017) 1671–1676, https://doi.org/10.1007/s00170-017-0239-8.
[3] A.J. Sheoran, H. Kumar, P.K. Arora, G. Moona, Bio-medical applications of additive manufacturing: a review, Procedia Manuf. 51 (2020) 663–670, https://doi.org/10.1016/j.promfg.2020.10.093.
[4] K. Markandan, R. Lim, P.K. Kanaujia, I. Seetoh, M.R. Bin Mohd Rosdi, Z.H. Tey, J. S. Goh, Y.C. Lam, C. Lai, Additive manufacturing of composite materials and

functionally graded structures using selective heat melting technique, J. Mater. Sci. Technol. 47 (2000) 243–252, https://doi.org/10.1016/j.jmst.2019.12.016.
[5] P.J. Bartolo, Stereolithographic processes, in: Stereolithography, Springer, Boston, MA, 2011, pp. 1–36.
[6] R. Brighenti, L. Marsavina, M.P. Marghitas, M.P. Cosma, M. Montanari, Mechanical characterization of additively manufactured photopolymerized polymers, Mech. Adv. Mater. Struct. (2022) 1–12, https://doi.org/10.1080/15376494.2022.2045655.
[7] R. Brighenti, M.P. Cosma, L. Marsavina, A. Spagnoli, M. Terzano, Laser-based additively manufactured polymers: a review on processes and mechanical models, J. Mater. Sci. 56 (2) (2021) 961–998, https://doi.org/10.1007/s10853-020-05254-6.
[8] A.A. Ahmed, L. Susmel, A material length scale–based methodology to assess static strength of notched additively manufactured polylactide (PLA), Fat. Fract. Eng. Mater. Struct. 41 (10) (2018) 2071–2098, https://doi.org/10.1111/ffe.12746.
[9] A.A. Ahmed, L. Susmel, Static assessment of plain/notched polylactide (PLA) 3D-printed with different infill levels: Equivalent homogenised material concept and Theory of Critical Distances, Fat. Fract. Eng. Mater. Struct. 42 (4) (2019) 883–904, https://doi.org/10.1111/ffe.12746.
[10] F. Arbeiter, M. Spoerk, J. Wiener, et al., Fracture mechanical characterization and lifetime estimation of near homogeneous components produced by fused filament fabrication, Polym. Test. 66 (2018) 105–113, https://doi.org/10.1016/j.polymertesting.2018.01.002.
[11] C. Vălean, L. Marşavina, M. Mărghitaş, et al., The effect of crack insertion for FDM printed PLA materials on Mode I and Mode II fracture toughness, Procedia Struct. Integrity 28 (2020) 1134–1139, https://doi.org/10.1016/j.prostr.2020.11.128.
[12] E. Linul, L. Marsavina, D.I. Stoia, Mode I and II fracture toughness investigation of Laser-Sintered Polyamide, Theor. Appl. Fract. Mech. 106 (2020), https://doi.org/10.1016/j.tafmec.2020.102497.
[13] D.I. Stoia, L. Marsavina, E. Linul, Mode I fracture toughness of polyamide and alumide samples obtained by Selective Laser Sintering additive process, Polymers 12 (2020) 640, https://doi.org/10.3390/polym12030640.
[14] A. Lubatsch, J. Kroha, K. Busch, Theory of light diffusion in disordered media with linear absorption or gain, Phys. Rev. B 71 (18) (2005), https://doi.org/10.1103/PhysRevB.71.184201.
[15] R. Brighenti, M.P. Cosma, L. Marsavina, A. Spagnoli, M. Terzano, Multiphysics modelling of the mechanical properties in polymers obtained via photo-induced polymerization, Int. J. Adv. Manuf. Technol. 117 (1) (2021) 481–499, https://doi.org/10.1007/s00170-021-07273-2.
[16] J. Wu, Z. Zhao, C.M. Hamel, X. Mu, X. Kuang, Z. Guo, H.J. Qi, Evolution of material properties during free radical photopolymerization, J. Mech. Phys. Solids 112 (2018) 25–49, https://doi.org/10.1016/j.jmps.2017.11.018.
[17] M. Zarrelli, A.A. Skordos, I.K. Partridge, Toward a constitutive model for cure-dependent modulus of a high temperature epoxy during the cure, Eur. Polym. J. 46 (8) (2010) 1705–1712, https://doi.org/10.1016/j.eurpolymj.2010.06.002.
[18] R. Brighenti, M.P. Cosma, Mechanical behavior of photopolymerized materials, J. Mech. Phys. Solids 153 (2021), https://doi.org/10.1016/j.jmps.2021.104456.
[19] ISO 527-1:2019. Plastics — Determination of tensile properties — Part 1: General principles.
[20] ASTM D 5045–14: Standard Test Methods for Plane-Strain Fracture Toughness and Strain Energy Release Rate of Plastic Materials.
[21] Aznarte, E., Ayranci, C., Qureshi, A.J. Digital Light Processing: Anisotropic tensile considerations, Proceedings of the 28th Annual International Solid Freeform Fabrication Symposium – An Additive Manufacturing Conference, 2017, 413-425.
[22] H. Masuda, K. Iinoya, Theoretical study of the scatter of experimental data due particle-sie-distribution, J. Chem. Eng. Jpn. 4 (1) (1971) 60–66, https://doi.org/10.1252/jcej.4.60.